NRL Report 6692

# Measurements of the Solar Brightness Distribution at 14.50 GHZ

J. P. Hollinger

*E. O. Hulburt Center for Space Research*

June 6, 1968

NAVAL RESEARCH LABORATORY
Washington, D.C.

This document has been approved for public release and sale; its distribution is unlimited.

CONTENTS


| | |
|---|---|
| Abstract | ii |
| Problem Status | ii |
| Authorization | ii |
| INTRODUCTION | 1 |
| SOLAR ACTIVITY | 1 |
| SPECTRA OF SOLAR ACTIVITY | 1 |
| BRIGHTNESS DISTRIBUTION CENTROID | 3 |
| EQUIPMENT AND MEASUREMENT PROCEDURE | 5 |
| RESULTS | 9 |
| ACKNOWLEDGMENTS | 9 |
| REFERENCES | 13 |
| APPENDIX A - Computer Program for Data Reduction | 14 |

## ABSTRACT

Observations of the solar brightness distribution at 14.50 GHz have been made using the NRL 85-ft reflector. The apparent angular size, intensity, and relative position of the active regions present on the solar disk were measured on six different days. These measurements were used to compute the radio brightness centroid relative to the geometrical center of the solar disk and the flux and size of the active regions. Spectral corrections were applied to the data to derive the brightness centroid at 15.375 GHz.


## PROBLEM STATUS

This is a final report on one phase of the problem; work continues on the problem.

## AUTHORIZATION

NRL Problem A01-35
Project S-3404, Task 4896


Manuscript submitted January 10, 1968.

# MEASUREMENTS OF THE SOLAR BRIGHTNESS DISTRIBUTION AT 14.50 GHZ

## INTRODUCTION

This project was initiated to make measurements of the radio brightness distribution of the sun and to determine from these observations the radio centroid relative to the geometrical solar disk at times specified by the Naval Applied Science Laboratory to be concurrent with certain operational requirements.

The radio sun often exhibits enhanced radio radiation in the form of spots or bursts which appear superimposed upon the uniformly bright disk of the quiet sun. Though the time of occurrence of individual activity is unpredictable, the average solar activity varies cyclically with a period of about 11 years. We are now entering the period of maximum activity. The activity can distort the radio brightness distribution of the sun such as to displace the radio brightness center from the center of the solar disk.

The monitor observations were made at 14.50 GHz using the NRL 85-ft reflector. To date, the sun has been monitored on six different days: October 10, 11, 12, and 13 and November 6 and 7. Further monitor observations are planned for the near future.

## SOLAR ACTIVITY

At frequencies near 15 GHz, in the absence of sunspots and bursts, the quiet sun appears as a nearly uniform, bright circular disk of roughly the same angular diameter as that of the sun's chromosphere, approximately 32 arc min (1). At frequencies between 10 GHz and 30 GHz sunspots appear as small-diameter regions of relatively intense radiation superimposed on the solar disk and consist of an intense nucleus with an angular diameter of about 2 arc min or less surrounded by a less intense region of angular diameter between 4 and 8 arc min (1). The average effective angular diameter of 46 sunspot regions at 14.50 GHz measured at NRL during this project was 2.1 arc min with sizes ranging up to 4.4 arc min. The 15-GHz flux from sunspots is typically a few percent or less than that of the quiet sun (1). Sunspots have lifetimes that vary from less than a day to several months, but typical spots have lifetimes ranging from 1 to 10 days (2a). Solar bursts, as differentiated from the slowly varying spot radiation, also appear as regions of intense radiation superimposed on the solar disk, and at 15 GHz they probably have angular diameters ranging from about 1 to 2 arc min, but they may be 10 times or greater than 100 times more intense than spot radiation (1). Bursts have lifetimes ranging from a few minutes to a few hours with the shorter-lived bursts being the most numerous (1).

## SPECTRA OF SOLAR ACTIVITY

The monitor observations described here were made at 14.50 GHz, but a knowledge of the brightness centroid was desired at the nearby frequency of 15.375 GHz.

It has been found that, at least over limited frequency ranges, the radiation spectra of most phenomena in radio astronomy are power spectra of the form

$$S = cf^{x} , \tag{1}$$

where $S$ is the flux density of the radiation (the power received at the earth per unit area per unit frequency interval), $c$ is a proportionality constant, $f$ is the frequency of the radiation, and the exponent $x$ is called the spectral index. Therefore, the ratio of the flux densities $S_1/S_2$ at frequencies $f_1$ and $f_2$ is given by

$$S_1/S_2 = (f_1/f_2)^{x} . \tag{2}$$

The quiet-sun radiation varies very slowly with a period of 11 years and is nearly constant over periods of several years (1). The spectral index of the quiet-sun radiation at frequencies near 15 GHz during the period of sunspot maximum is $x = +1.3$ (2b). Therefore, the predicted ratio of the flux density of the quiet-sun radiation at 14.50 GHz to the flux density at 15.375 GHz is 0.927.

The spectral index of the radiation from sunspots in the frequency range from 4 GHz to 17 GHz is approximately $x = -0.7$ (1a,3). Therefore, the predicted ratio of the flux density of sunspot radiation at 14.50 GHz to that at 15.375 GHz is 1.042.

The flux density of the radiation from solar bursts at frequencies near 15 GHz is nearly independent of frequency (1b,4). Therefore, the spectral index is zero and the flux-density ratio at 14.50 GHz and 15.375 GHz is 1.000.

From the above values the ratio of the flux from a sunspot to the flux from the quiet sun at 15.375 GHz is less than the same ratio at 14.50 GHz by a factor of 0.927/1.042 = 0.89. The ratio of the flux from a burst to the flux from the quiet sun at 15.375 GHz is less than the same ratio at 14.50 GHz by a factor of 0.927/1.000 = 0.93.

The centroid of the flux distribution of the active sun relative to the geometrical center of the quiet sun is given by (see following section)

$$\overline{\theta} = \frac{\int_D \theta_D \, dS_D(\theta)/S_Q}{1 + (S_D/S_Q)} , \tag{3}$$

where $\theta_D$ is the distance from the geometrical center of the solar disk to the disturbance, $dS_D(\theta)$ is the flux of the disturbance at $\theta_D$ and $S_D$ and $S_Q$ are the total fluxes of the disturbance and the quiet sun, respectively. For disturbances whose angular diameters are small compared to the disk of the sun (as are spots and bursts),

$$\overline{\theta} \cong \frac{\theta_D(S_D/S_Q)}{1 + (S_D/S_Q)} . \tag{4}$$

Hence, for a disturbance whose flux is small compared to the quiet-sun flux,

$$\overline{\theta} \cong \theta_D(S_D/S_Q) , \tag{5}$$

and the displacement of the centroid is proportional to the ratio of the fluxes of the disturbance and the quiet sun.

Therefore, it is estimated that sunspots will shift the apparent radio centroid from the sun's true center at 14.50 GHz by an angle that does not differ from the shift at 15.375 GHz by more than about 11%, while shifts in the centroid due to bursts will differ at the two frequencies by not more than about 7%. In each case the shift will be such as

to displace the centroid at 14.50 GHz more than at 15.375 GHz. A correction, based on the above discussion, has been applied using the known average spectra to correct for this error and reduce it to a negligible amount.

## BRIGHTNESS DISTRIBUTION CENTROID

The centroid position $(\bar{\alpha}, \bar{\delta})$ of the brightness temperature distribution $T_B(\alpha, \delta)$ is defined as

$$\bar{\alpha} = \frac{\int \alpha T_B(\alpha, \delta)\, d\alpha d\delta}{\int T_B(\alpha, \delta)\, d\alpha d\delta} . \tag{6}$$

The definition of the orthogonal coordinate $\bar{\delta}$ parallels that of $\bar{\alpha}$, as does the analytical development which follows. Therefore, only the equations for $\bar{\alpha}$ will be written explicitly.

The quantity actually observed is the antenna temperature distribution $T_A(\alpha, \delta)$ and not $T_B(\alpha, \delta)$. They are related by

$$T_A(\alpha, \delta) = \frac{N_{MB}}{\Omega_{MB}} \int_{MB} f(\theta, \varphi)\, T_B(\theta + \alpha, \varphi + \delta)\, d\theta d\varphi , \tag{7}$$

where $f(\theta, \varphi)$ is the antenna response pattern, $f(0, 0) = 1$, and $N_{MB}$ and $\Omega_{MB}$ are the main-beam efficiency and the main-beam solid angle of the antenna, respectively. They are related by

$$\Omega_{MB} = \int_{MB} f(\theta, \varphi)\, d\theta d\varphi \tag{8}$$

and

$$N_{MB} = \frac{\epsilon A_g \Omega_{MB}}{\lambda^2} , \tag{9}$$

where $\lambda$ is the wavelength of the radiation and $\epsilon$ and $A_g$ are the aperture efficiency and the geometrical area of the antenna, respectively.

If the antenna response pattern is very narrow compared to the size of the smallest detail of the solar brightness temperature distribution, Eq. (7) immediately gives

$$T_B(\alpha, \delta) = \frac{T_A(\alpha, \delta)}{N_{MB}} . \tag{10}$$

The measured antenna temperature distribution then differs from the true brightness temperature distribution only by a proportionality constant and can be substituted into Eq. (6) and the centroid calculated directly. This, of course, is not the case. The half-power beamwidth of the 85-ft antenna at 14.50 GHz is 3.3 arc min, and spot and burst solar activity are typically of comparable extent. However, the beamwidth is small compared to the size of the solar disk (about 32 arc min), and very little error in the centroid is incurred by a lack of knowledge concerning the exact detail of structure too small to be resolved by the 3.3-arc min beam. In fact, if the structure is symmetric about its center, no error is imposed by the finite resolution.

A first-order approximation to the shape of solar activity is that it has a Gaussian distribution given by

$$T_B(\alpha, \delta)_i = T_{Bi} \exp\left\{\frac{-4 \ln 2 \ [(\alpha - \alpha_i)^2 + (\delta - \delta_i)^2]}{W_i^2}\right\}, \tag{11}$$

where $T_{Bi}$ is the peak brightness temperature and $W_i$ is the half-power width of the $i$th active region, which is located at $(\alpha_i, \delta_i)$. The main-beam antenna response pattern is nearly Gaussian and, to a good approximation, is given by

$$f(\theta, \varphi) = \exp\left[\frac{-4 \ln 2 \ (\theta^2 + \varphi^2)}{W_B^2}\right], \tag{12}$$

where $W_B$ is the half-power beamwidth. Using Eqs. (7), (11), and (12), and taking the integration limits as infinite, which introduces negligible error, the measured antenna temperature of the $i$th spot is

$$T_A(\alpha, \delta)_i = \frac{N_{MB} \ T_{Bi}}{[1 + (W_B^2/W_i^2)]} \exp\left\{\frac{-4 \ln 2 \ [(\alpha - \alpha_i)^2 + (\delta - \delta_i)^2]}{(W_i^2 + W_B^2)}\right\}, \tag{13}$$

If this measured antenna temperature distribution is taken as the true brightness distribution of the active regions, Eq. (6) gives the centroid of a collection of active regions superimposed on the quiet sun as

$$\bar{\alpha} = \frac{\sum_i \left(\frac{\pi W_i^2}{4 \ln 2}\right) T_{Bi} \alpha_i}{T_{B\,\mathrm{sun}} \pi R_{\mathrm{sun}}^2 + \sum_i \left(\frac{\pi W_i^2}{4 \ln 2}\right) T_{Bi}}, \tag{14}$$

where $T_{B\,\mathrm{sun}}$ and $R_{\mathrm{sun}}$ are the brightness temperature and the radius of the solar disk, and the summation is over all the active regions present. The origin of the $(\alpha, \delta)$ coordinate systems has been chosen at the geometrical center of the solar disk in order to make the contribution of the quiet sun to the integral in the numerator of Eq. (6) zero, and use has been made of the fact that the quiet solar disk is well resolved by the antenna beam.

The resolution of the antenna does not appear in Eq. (14), and the result is identical to that obtained by using the true brightness distribution given by Eq. (11). All that is required is that the resolution be sufficiently narrow to allow accurate determination of the peak intensity, size, and relative position of the active regions. This condition is adequately fulfilled by the 3.3-arc-min beam.

The centroid given by Eq. (14) can be expressed in terms of observable quantities by using the equation for the flux $S$ from a source given by

$$S = \frac{2k}{\lambda^2} \int_{\text{source}} T_B(\alpha, \delta) \, d\alpha d\delta \equiv \frac{2k}{\lambda^2 N_{MB}} \int_{\text{source}} T_A(\alpha, \delta) \, d\alpha d\delta, \tag{15}$$

where $k$ is Boltzmann's constant. Using Eqs. (11), (13), and (15),

$$S_{sun} = \frac{2kT_{Bsun}\,\pi R_{sun}^2}{\lambda^2} = \frac{2kT_{Asun}\,\pi R_{sun}^2}{\lambda^2 N_{MB}}$$

and (16)

$$S_i = \frac{2kT_{Bi}\,\pi W_i^2}{\lambda^2 4\,ln\,2} = \frac{2kT_{Ai}\,\pi(W_i^2 + W_B^2)}{\lambda^2 N_{MB}\,4\,ln\,2}\,,$$

and Eq. (14) may be written as

$$\bar{\alpha} = \frac{\sum_i (S_i/S_{sun})\,\alpha_i}{1 + \sum_i (S_i/S_{sun})}\,, \tag{17}$$

which is Eq. (3) used in the previous section. The quantity $(W_i^2 + W_B^2)$ is the square of the measured half-power response width $WR_i^2$ of the active region and indicates the apparent broadening of the region imposed by the resolution of the antenna. The flux ratio of the active regions to the quiet sun is given by Eq. (16) as

$$\frac{S_i}{S_{sun}} = \frac{T_{Ai}\,WR_i^2}{T_{Asun}\,4\,ln\,2R_{sun}^2}\,. \tag{18}$$

Thus, to calculate the centroid position using Eqs. (17) and (18), it is necessary to measure the antenna temperature and response width of each active region and its position relative to the geometrical center of the quiet sun, and the antenna temperature and radius of the quiet solar disk.

## EQUIPMENT AND MEASUREMENT PROCEDURE

The equipment used consisted of a conventional Dicke-type crystal-mixer receiver and the NRL 85-ft reflector.

The receiver accepted radiation in two bands each 13 MHz wide and symmetrically disposed on either side of the local oscillator frequency of 14.50 GHz by the 43-MHz i-f frequency. A 1-sec-integration time constant was used. The system was sensitive to linearly polarized radiation at a 0-degree position angle (i.e., north-south).

The 85-ft antenna was focused using Venus as a source. Venus was also used to measure the half-power beamwidth of the antenna. It was determined to be the same in both right ascension and declination within the error of measurement, with a value of 3.3 ± 0.1 arc min. The diameter of Venus at the time of these calibration measurements was 0.8 arc min.

Linearity of the system response to signals in the intensity range of the quiet sun was checked by inserting attenuation in the signal line before the i-f amplifier, using a calibrated precision attenuator while tracking the sun with the antenna. The linearity was found to be better than 1% for signals up to five times the quiet sun and better than 5% for signals up to ten times the quiet sun. The antenna temperature of the sun was calibrated by replacing the feed horn at the focus of the 85-ft reflector by an argon-discharge noise source with an equivalent noise temperature of 12,000°K. The average quiet sun gave an antenna temperature of about 7000°K, which greatly exceeded the rms

output noise fluctuations of the system while observing the sun of approximately 3°K. The efficiency of the 85-ft reflector at 14.50 GHz was previously found to be 0.49 ± 0.05 (5).

Data were taken both in analog form on a pen recorder and digitally on IBM cards. The observations consisted of 5-min drift scans with the antenna set at a preselected declination and the sun allowed to drift through the antenna beam due to the earth's rotation. A set of observations on a given day consisted of a series of 13 drift scans of the sun taken at intervals of 3 arc min in declination to form a raster covering the solar disk. The scan through the center was taken first followed by scans alternately south and then north up to 18 arc min south and north of the center. Between drift scans the apparent declination of the center of the sun was found by a declination scan. These declination scans were at the same scan rate as the drift scans and were taken while tracking the right ascension of the solar center, as determined from the previous drift scan. In this manner the apparent right ascension and declination of the solar center were determined periodically throughout the observations, and at any time it was possible to predict accurately the apparent declination of the solar center for the next scan. All measurements were therefore relative to the apparent geometrical center of the solar disk, and no absolute position measurements were made. Figure 1 shows a typical set of pointing data taken during a set of observations. The solid lines are the predicted absolute solar coordinates with no corrections for refraction or pointing of the antenna applied; the points are the measured coordinates, and the dashed lines are the best fit to the data of the apparent solar coordinates as a function of local hour angle. As can be seen, the apparent coordinates of the solar center were monitored to an accuracy of about 0.1 arc min in declination and about 1 sec in right ascension (0.2 to 0.3 arc min).

As these scans were being taken, the approximate coordinates, relative to the solar center, of any active regions present and a rough estimate of their intensity, were recorded. It should be noted that, with the scan interval of 3 arc min and the 3.3-arc min beam, all active regions present would appear during the scan set to at least half intensity, so that none would be missed. After completing the scan set, each active region was observed independently by right ascension and declination scans through the position of peak intensity. These scans were at one-half the rate used for the scan set, to enable improved measurement accuracy. The apparent coordinates of the solar center were measured periodically, as was done during the scan set.

This series of observations required about 4 hours. The observations were generally started 2 hours before solar transit to center them on the local meridian. This minimized the maximum local hour angle of the observations and thus tended to minimize refraction and atmospheric absorption effects. The performance characteristics of the antenna, such as pointing, tracking, and efficiency, are also optimum near the meridian. The monitor observations, therefore, refer to solar conditions at about noon EST of the date on which they were made.

On only one day, October 10, when the data were taken in a heavy rain, did the apparent antenna temperature of the quiet sun vary during the observations. A relative correction, derived from the quiet sun deflection, was applied to the data to correct for the varying atmospheric absorption.

The antenna temperature and the radius of the quiet solar disk, the response width, the antenna temperature, and the coordinates relative to the center of the sun for each active region were measured from the analog chart recordings. Errors in each quantity were conservatively estimated and are given as standard errors. These data were then used to compute the centroid position from Eqs. (17) and (18). The fluxes of the individual regions were calculated from Eq. (16) using Eqs. (8), (9), and (12), and the size of the regions was found from $W_i = (WR_i^2 - W_B^2)^{1/2}$. Errors were calculated according to the standard propagation-of-errors equation applied to these equations. The computer program used for the computation is given in Appendix A.

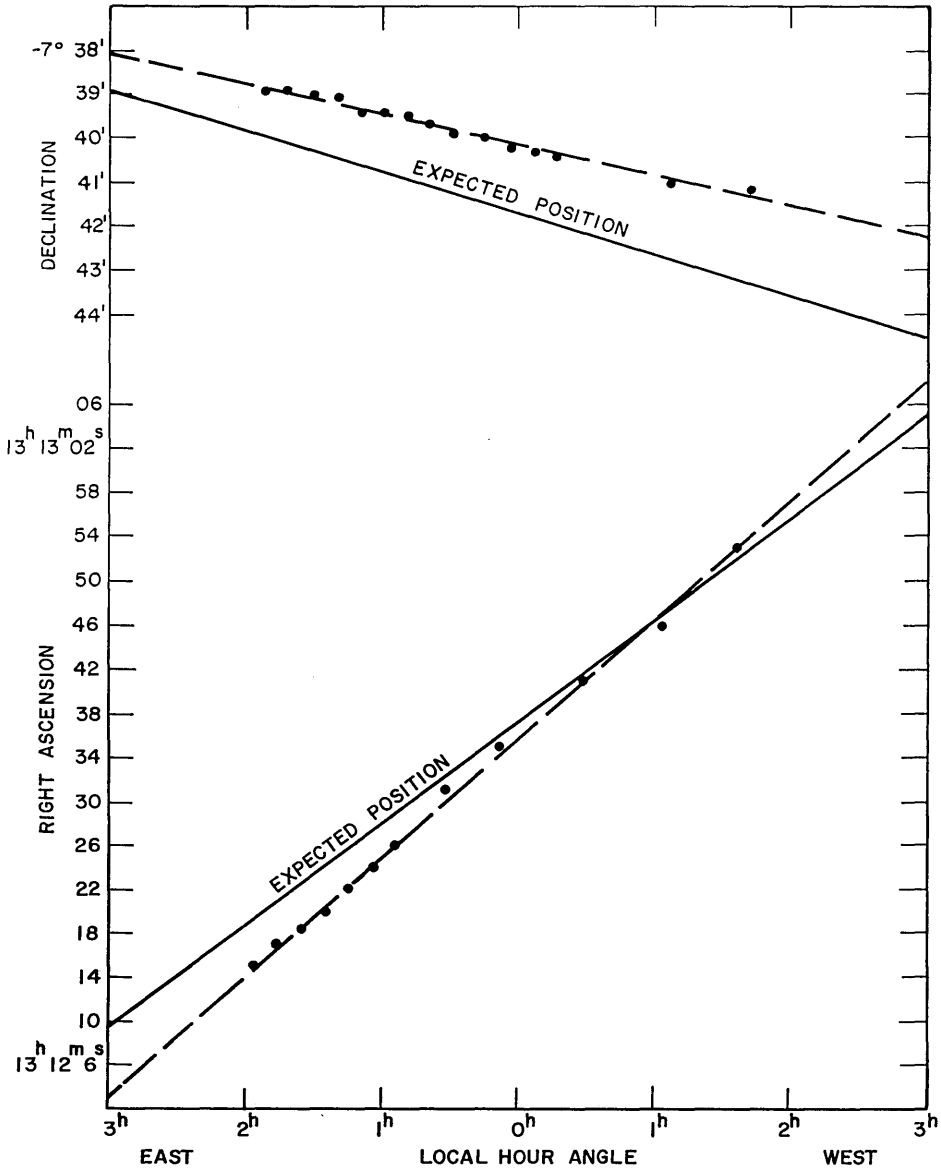


Fig. 1 - Solar pointing data for October 13, 1967

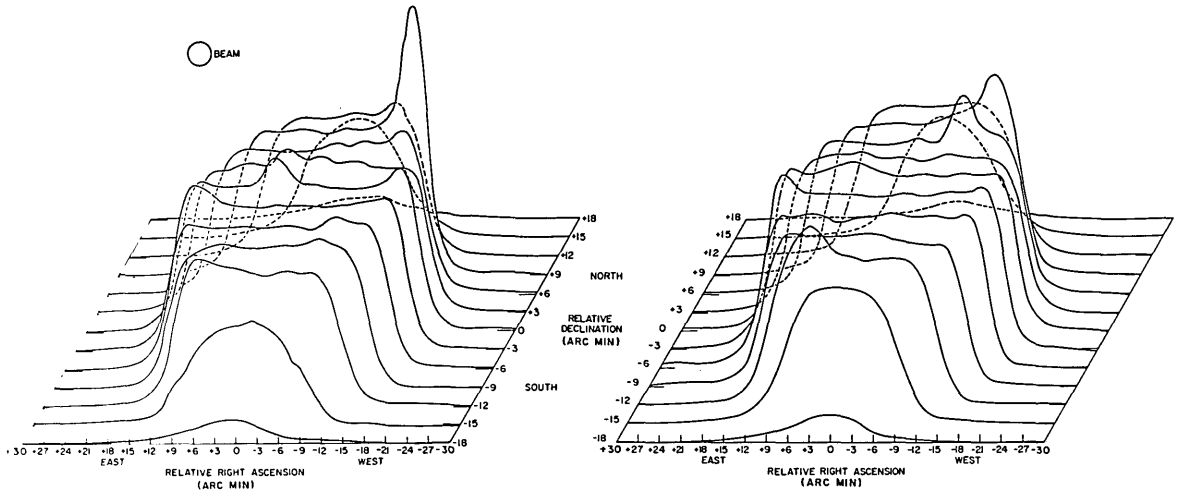


(a) Sun at 14.50 GHz on October 10, 1967

(d) Sun at 14.50 GHz on October 13, 1967

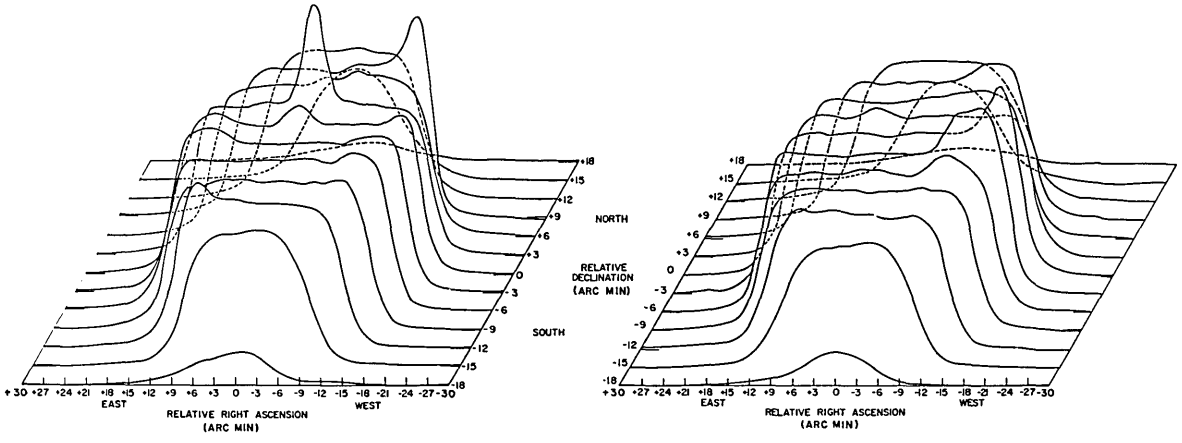


(b) Sun at 14.50 GHz on October 11, 1967

(e) Sun at 14.50 GHz on November 6, 1967

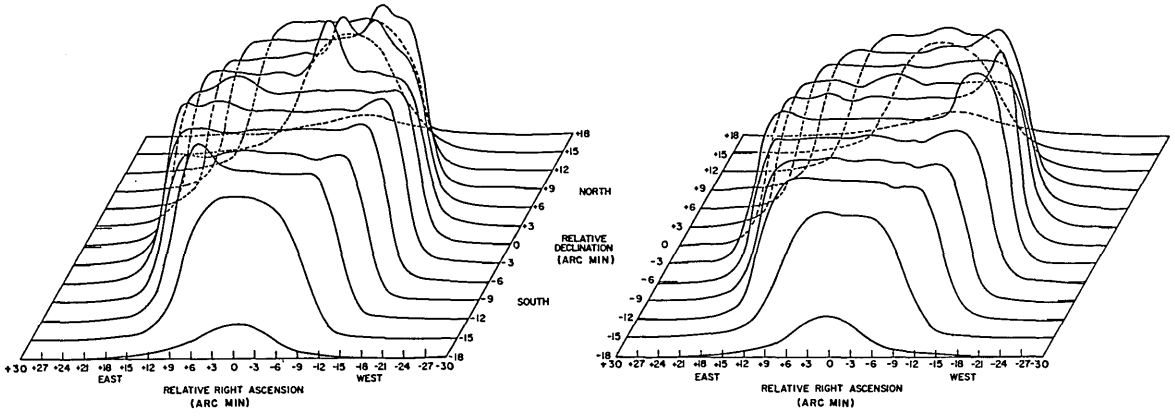


(c) Sun at 14.50 GHz on October 12, 1967

(f) Sun at 14.50 GHz on November 7, 1967

Fig. 2 - Tracings of the 13 actual drift-scan recordings taken to form a raster covering the solar disk

## RESULTS

A qualitative picture of the solar brightness distribution on the six days in which monitor observations were made is shown in Fig. 2. Each figure is composed of tracings of the 13 actual drift-scan recordings taken to form a raster covering the solar disk. The scans have been separated, and skewed for clarity, in a vertical direction by an amount appropriate for the 3.0-arc min declination interval at which they were taken. Right ascension and declination coordinates relative to the center of the solar disk are given, and a circle representing the 3.3-arc min beamwidth is shown. The sun was never observed as a uniformly bright circular disk; sunspots were always present. The most intense spot observed was on the northwest solar limb on October 10, with a flux of 2.2% that of the quiet sun. The weakest spot that could be detected had a flux of about 0.1% of the solar flux. No solar bursts were observed.

The details of the observations are given in Tables 1 through 6, which present the results from the computer program given in Appendix A. The measured values for the output deflection and the radius of the quiet sun, and the output deflection, the response width, and the position relative to the center of the solar disk for the individual sunspots, as well as the estimated error in each of these quantities, are presented in the left halves of the tables. The output deflections are in inches on the analog output chart recording and can be converted to antenna temperature by using the result of the argon-discharge noise calibration described previously. From this calibration an output deflection of 1 in. is equivalent to a 1750°K antenna temperature. The computed quantities are listed next. The computed quantities for the individual sunspots are: the ratio of the flux of the sunspot to the flux from the quiet sun and its error in percent, the angular size of the sunspot and its error in arc min, and the flux of the sunspot in janskys (one jansky is $10^{-26}$ w/m$^2$-Hz) and its error in percent. The right ascension and declination coordinates of the brightness centroid relative to the center of the solar disk were computed at 14.50 GHz and at 15.375 GHz using a spectral correction of 0.89, as discussed previously. The centroid position was also computed in polar coordinates at 15.375 GHz. The radial distance from the geometrical center of the sun to the centroid of the brightness distribution is given in arc sec, and its position angle measured from the north point of the sun counterclockwise through east is given in angular degrees.

The maximum displacement of the centroid observed during the six days to date was 14.7 ± 4.7 arc sec, and the minimum displacement was 3.8 ± 1.4 arc sec. The average displacement was about 9 arc sec. The average error in the centroid position was about 3 arc sec, which is less than 0.2% the size of the solar disk.

## ACKNOWLEDGMENTS

Most of the members of the Radio Astronomy Branch have contributed to this project in some way, and I am grateful for their assistance. In particular, I thank R. M. Sloanaker for his contributions in the determination of the relevant solar physics of the project and him and J. M. Bologna for conducting the observations and data reduction on November 6 and 7. Special thanks are extended to S. R. MacLeod for his responsibility in the construction, testing, and installation of the radiometer and for his assistance in making the observations and reducing the data.

## Table 1
## Sun Data on Oct. 10, 1967, at 14.50 GHz Using the 85-ft Maryland Point Telescope

| Sun Deflection | Sun Radius (min) | Avg Sun Declination (deg) | Hotspots Present | | | | | | | | | Position of Brightness Centroid at 14.50 GHz Relative to Sun's Geometric Center | | Centroid at 15.375 GHz Using Spectral Correction of 0.89 | | Centroid at 15.375 GHz Expressed in Polar Coordinates | |
|---|---|---|---|---|---|---|---|---|---|---|---|---|---|---|---|---|---|
| | | | | Measured Quantities | | | | Computed Quantities | | | | | | | | | |
| | | | Hotspot No. | Deflection | Width (min) | Right Ascension (min) | Declination (min) | Ratio of Flux to Quiet Sun Flux (%) | Size (min) | Flux (jansky) | Error in Flux Value (± %) | R.A. (arc sec) | Decl. (arc sec) | R.A. (arc sec) | Decl. (arc sec) | Radius (arc sec) | Position Angle (deg) |
| 4.05 ± 0.05 | 16.5 ± 0.5 | -6.55 | 1 | 4.90 ± 0.20 | 3.7 ± 0.5 | -11.4 ± 0.2 | 9.1 ± 0.2 | 2.19 ± 0.61 | 1.7 ± 1.4 | .103 | 27 | -11.8 ± 4.5 | 9.9 ± 3.5 | -10.5 ± 4.5 | 8.8 ± 3.5 | 13.7 ± 4.1 | 309.9 ± 16.5 |
| | | | 2 | 0.57 ± 0.07 | 3.4 ± 0.1 | -14.2 ± 0.5 | -0.1 ± 0.2 | 0.22 ± 0.04 | 0.8 ± 0.7 | 11,306 | 15 | | | | | | |
| | | | 3 | 1.10 ± 0.10 | 3.5 ± 0.2 | 2.5 ± 0.2 | 1.8 ± 0.2 | 0.44 ± 0.07 | 1.2 ± 0.8 | 23,121 | 15 | | | | | | |
| | | | 4 | 0.65 ± 0.10 | 5.1 ± 1.0 | 12.9 ± 0.7 | -1.3 ± 0.4 | 0.55 ± 0.24 | 3.9 ± 1.4 | 29,009 | 42 | | | | | | |
| | | | 5 | 0.30 ± 0.05 | 3.7 ± 0.8 | -6.2 ± 0.5 | 5.5 ± 0.3 | 0.13 ± 0.07 | 1.7 ± 1.9 | 7,047 | 49 | | | | | | |
| | | | 6 | 0.35 ± 0.05 | 4.1 ± 0.8 | -2.2 ± 0.5 | 4.8 ± 0.3 | 0.19 ± 0.09 | 2.4 ± 1.9 | 10,095 | 44 | | | | | | |
| | | | 7 | 0.30 ± 0.10 | 4.0 ± 1.3 | -8.2 ± 1.0 | -6.6 ± 1.0 | 0.16 ± 0.12 | 2.3 ± 2.5 | 8,236 | 75 | | | | | | |
| | | | 8 | 0.30 ± 0.15 | 3.6 ± 0.3 | 8.2 ± 1.5 | -12.0 ± 1.5 | 0.13 ± 0.07 | 1.4 ± 1.1 | 6,671 | 53 | | | | | | |
| | | | 9 | 0.20 ± 0.15 | 5.0 ± 1.3 | 5.5 ± 1.5 | -12.0 ± 1.5 | 0.16 ± 0.15 | 3.8 ± 2.5 | 8,579 | 92 | | | | | | |

## Table 2
## Sun Data on Oct. 11, 1967, at 14.50 GHz Using the 85-ft Maryland Point Telescope

| Sun Deflection | Sun Radius (min) | Avg Sun Declination (deg) | Hotspots Present | | | | | | | | | Position of Brightness Centroid at 14.50 GHz Relative to Sun's Geometric Center | | Centroid at 15.375 GHz Using Spectral Correction of 0.89 | | Centroid at 15.375 GHz Expressed in Polar Coordinates | |
|---|---|---|---|---|---|---|---|---|---|---|---|---|---|---|---|---|---|
| | | | | Measured Quantities | | | | Computed Quantities | | | | | | | | | |
| | | | Hotspot No. | Deflection | Width (min) | Right Ascension (min) | Declination (min) | Ratio of Flux to Quiet Sun Flux (%) | Size (min) | Flux (jansky) | Error in Flux Value (± %) | R.A. (arc sec) | Decl. (arc sec) | R.A. (arc sec) | Decl. (arc sec) | Radius (arc sec) | Position Angle (deg) |
| 4.14 ± 0.05 | 16.7 ± 0.5 | -6.92 | 1 | 3.00 ± 0.05 | 3.7 ± 0.3 | -1.0 ± 0.2 | 3.5 ± 0.2 | 1.28 ± 0.22 | 1.7 ± 0.7 | 70,471 | 17 | -2.3 ± 1.8 | 3.6 ± 1.2 | -2.0 ± 1.8 | 3.2 ± 1.2 | 3.8 ± 1.4 | 328.1 ± 25.4 |
| | | | 2 | 0.58 ± 0.07 | 4.8 ± 0.5 | 10.5 ± 0.5 | -1.5 ± 0.3 | 0.42 ± 0.11 | 3.5 ± 0.8 | 22,929 | 26 | | | | | | |
| | | | 3 | 0.55 ± 0.15 | 3.3 ± 0.7 | 8.7 ± 0.7 | -12.5 ± 0.5 | 0.19 ± 0.10 | 0.0 ± 1.7 | 10,277 | 50 | | | | | | |
| | | | 4 | 1.10 ± 0.15 | 3.4 ± 0.5 | -11.4 ± 0.7 | 9.1 ± 0.5 | 0.40 ± 0.13 | 0.8 ± 1.4 | 21,819 | 32 | | | | | | |
| | | | 5 | 0.35 ± 0.15 | 4.5 ± 1.2 | -14.4 ± 0.7 | -0.5 ± 0.5 | 0.22 ± 0.15 | 3.1 ± 2.3 | 12,161 | 68 | | | | | | |
| | | | 6 | 0.30 ± 0.15 | 4.5 ± 1.2 | -4.7 ± 0.7 | 6.2 ± 0.5 | 0.19 ± 0.14 | 3.1 ± 2.3 | 10,424 | 73 | | | | | | |

## Table 3
## Sun Data on Oct. 12, 1967, at 14.50 GHz Using the 85-ft Maryland Point Telescope

| Sun Deflection | Sun Radius (min) | Avg Sun Declination (deg) | Hotspots Present | | | | | | | | | Position of Brightness Centroid at 14.50 GHz Relative to Sun's Geometric Center | | Centroid at 15.375 GHz Using Spectral Correction of 0.89 | | Centroid at 15.375 GHz Expressed in Polar Coordinates | |
|---|---|---|---|---|---|---|---|---|---|---|---|---|---|---|---|---|---|
| | | | | Measured Quantities | | | | Computed Quantities | | | | | | | | | |
| | | | Hotspot No. | Deflection | Width (min) | Right Ascension (min) | Declination (min) | Ratio of Flux to Quiet Sun Flux (%) | Size (min) | Flux (jansky) | Error in Flux Value (± %) | R.A. (arc sec) | Decl. (arc sec) | R.A. (arc sec) | Decl. (arc sec) | Radius (arc sec) | Position Angle (deg) |
| 4.25 ± 0.10 | 16.5 ± 0.5 | -7.29 | 1 | 0.80 ± 0.15 | 3.7 ± 0.4 | 7.4 ± 0.7 | -12.5 ± 0.4 | 0.34 ± 0.10 | 1.7 ± 1.2 | 18,792 | 29 | -4.7 ± 1.7 | 3.9 ± 1.4 | -4.2 ± 1.7 | 3.5 ± 1.4 | 5.5 ± 1.6 | 309.7 ± 16.0 |
| | | | 2 | 0.30 ± 0.10 | 3.7 ± 0.4 | -13.4 ± 0.7 | -3.4 ± 0.4 | 0.13 ± 0.05 | 1.7 ± 1.2 | 7,047 | 40 | | | | | | |
| | | | 3 | 0.50 ± 0.10 | 4.6 ± 1.0 | 7.9 ± 0.5 | 0.1 ± 0.2 | 0.33 ± 0.16 | 3.2 ± 1.5 | 18,154 | 48 | | | | | | |
| | | | 4 | 2.20 ± 0.15 | 3.6 ± 0.3 | -4.0 ± 0.5 | 4.7 ± 0.2 | 0.89 ± 0.17 | 1.4 ± 1.0 | 48,923 | 18 | | | | | | |
| | | | 5 | 1.35 ± 0.15 | 3.9 ± 0.6 | -8.3 ± 0.5 | 8.0 ± 0.3 | 0.64 ± 0.21 | 2.1 ± 1.5 | 35,233 | 33 | | | | | | |
| | | | 6 | 0.55 ± 0.15 | 3.8 ± 0.6 | -10.9 ± 1.0 | 8.5 ± 1.0 | 0.25 ± 0.10 | 1.9 ± 1.5 | 13,627 | 42 | | | | | | |

## Table 4
## Sun Data on Oct. 13, 1967, at 14.50 GHz Using the 85-ft Maryland Point Telescope

| Sun Deflection | Sun Radius (min) | Avg Sun Declination (deg) | Hotspots Present | | | | | | | | | Position of Brightness Centroid at 14.50 GHz Relative to Sun's Geometric Center | | Centroid at 15.375 GHz Using Spectral Correction of 0.89 | | Centroid at 15.375 GHz Expressed in Polar Coordinates | |
|---|---|---|---|---|---|---|---|---|---|---|---|---|---|---|---|---|---|
| | | | | Measured Quantities | | | | Computed Quantities | | | | | | | | | |
| | | | Hotspot No. | Deflection | Width (min) | Right Ascension (min) | Declination (min) | Ratio of Flux to Quiet Sun Flux (%) | Size (min) | Flux (jansky) | Error in Flux Value (± %) | R.A. (arc sec) | Decl. (arc sec) | R.A. (arc sec) | Decl. (arc sec) | Radius (arc sec) | Position Angle (deg) |
| 4.25 ± 0.10 | 16.5 ± 0.5 | -7.67 | 1 | 0.43 ± 0.07 | 5.4 ± 0.8 | 5.0 ± 0.5 | 1.2 ± 0.2 | 0.39 ± 0.13 | 4.3 ± 1.0 | 21,515 | 32 | -3.5 ± 2.3 | 2.8 ± 2.6 | -3.1 ± 2.3 | 2.5 ± 2.6 | 4.0 ± 2.4 | 309.4 ± 35.1 |
| | | | 2 | 0.55 ± 0.07 | 3.7 ± 0.5 | 14.4 ± 0.7 | -2.5 ± 0.4 | 0.23 ± 0.07 | 1.7 ± 1.4 | 12,919 | 30 | | | | | | |
| | | | 3 | 0.90 ± 0.20 | 4.4 ± 1.0 | 5.7 ± 0.7 | -12.2 ± 0.5 | 0.54 ± 0.28 | 2.9 ± 1.6 | 29,897 | 50 | | | | | | |
| | | | 4 | 1.70 ± 0.10 | 3.7 ± 0.3 | -7.1 ± 0.5 | 6.5 ± 0.2 | 0.73 ± 0.13 | 1.7 ± 0.6 | 39,934 | 17 | | | | | | |
| | | | 5 | 1.55 ± 0.10 | 4.0 ± 0.7 | -10.5 ± 0.7 | 9.2 ± 0.4 | 0.77 ± 0.28 | 2.3 ± 1.7 | 42,554 | 35 | | | | | | |
| | | | 6 | 0.20 ± 0.15 | 3.5 ± 0.3 | -13.9 ± 1.2 | -3.0 ± 1.0 | 0.08 ± 0.06 | 1.2 ± 1.1 | 4,203 | 77 | | | | | | |

## Table 5
## Sun Data on Nov. 6, 1967, at 14.50 GHz Using the 85-ft Maryland Point Telescope

| Sun Deflection | Sun Radius (min) | Avg Sun Declination (deg) | Hotspots Present | | | | | | | | | Position of Brightness Centroid at 14.50 GHz Relative to Sun's Geometric Center | | Centroid at 15.375 GHz Using Spectral Correction of 0.89 | | Centroid at 15.375 GHz Expressed in Polar Coordinates | |
|---|---|---|---|---|---|---|---|---|---|---|---|---|---|---|---|---|---|
| | | | | Measured Quantities | | | | Computed Quantities | | | | | | | | | |
| | | | Hotspot No. | Deflection | Width (min) | Right Ascension (min) | Declination (min) | Ratio of Flux to Quiet Sun Flux (%) | Size (min) | Flux (jansky) | Error in Flux Value (± %) | R.A. (arc sec) | Decl. (arc sec) | R.A. (arc sec) | Decl. (arc sec) | Radius (arc sec) | Position Angle (deg) |
| 3.80 ± 0.05 | 16.7 ± 0.5 | -15.93 | 1 | 2.10 ± 0.30 | 4.2 ± 0.6 | -13.7 ± 1.0 | -1.3 ± 1.0 | 1.26 ± 0.41 | 2.6 ± 1.0 | 63,563 | 32 | -16.5 ± 4.7 | 0.8 ± 3.0 | -14.7 ± 4.7 | 0.7 ± 3.0 | 14.7 ± 4.7 | 272.6 ± 11.6 |
| | | | 2 | 1.20 ± 0.30 | 4.0 ± 0.7 | -9.9 ± 1.0 | -3.1 ± 1.0 | 0.65 ± 0.28 | 2.3 ± 1.7 | 32,945 | 43 | | | | | | |
| | | | 3 | 0.70 ± 0.30 | 5.5 ± 1.8 | -8.4 ± 1.2 | 8.0 ± 1.0 | 0.72 ± 0.58 | 4.4 ± 3.1 | 36,334 | 79 | | | | | | |
| | | | 4 | 0.30 ± 0.10 | 3.8 ± 0.5 | 4.1 ± 0.7 | 2.6 ± 0.5 | 0.15 ± 0.06 | 1.9 ± 1.4 | 7,433 | 42 | | | | | | |
| | | | 5 | 0.10 ± 0.07 | 3.8 ± 0.5 | 1.0 ± 1.2 | -6.0 ± 1.6 | 0.05 ± 0.04 | 1.9 ± 1.4 | 2,477 | 74 | | | | | | |
| | | | 6 | 0.10 ± 0.07 | 3.8 ± 0.5 | 10.7 ± 1.2 | 6.0 ± 1.6 | 0.05 ± 0.04 | 1.9 ± 1.4 | 2,477 | 74 | | | | | | |
| | | | 7 | 0.10 ± 0.07 | 4.8 ± 1.5 | 1.0 ± 1.4 | 9.0 ± 1.6 | 0.08 ± 0.07 | 3.5 ± 2.7 | 3,953 | 93 | | | | | | |
| | | | 8 | 0.05 ± 0.04 | 3.3 ± 0.6 | -7.5 ± 1.2 | -12.0 ± 1.6 | 0.02 ± 0.02 | 0.0 ± 1.5 | 934 | 88 | | | | | | |
| | | | 9 | 0.15 ± 0.10 | 3.3 ± 0.5 | 7.7 ± 1.2 | -12.0 ± 1.6 | 0.06 ± 0.04 | 0.0 ± 1.4 | 2,802 | 73 | | | | | | |
| | | | 10 | 0.15 ± 0.10 | 3.6 ± 0.6 | -2.6 ± 1.2 | -15.0 ± 1.6 | 0.07 ± 0.05 | 1.4 ± 1.6 | 3,335 | 75 | | | | | | |

## Table 6
## Sun Data on Nov. 7, 1967, at 14.50 GHz Using the 85-ft Maryland Point Telescope

| Sun Deflection | Sun Radius (min) | Avg Sun Declination (deg) | Hotspots Present | | | | | | | | | Position of Brightness Centroid at 14.50 GHz Relative to Sun's Geometric Center | | Centroid at 15.375 GHz Using Spectral Correction of 0.89 | | Centroid at 15.375 GHz Expressed in Polar Coordinates | |
|---|---|---|---|---|---|---|---|---|---|---|---|---|---|---|---|---|---|
| | | | | Measured Quantities | | | | Computed Quantities | | | | | | | | | |
| | | | Hotspot No. | Deflection | Width (min) | Right Ascension (min) | Declination (min) | Ratio of Flux to Quiet Sun Flux (%) | Size (min) | Flux (jansky) | Error in Flux Value (± %) | R.A. (arc sec) | Decl. (arc sec) | R.A. (arc sec) | Decl. (arc sec) | Radius (arc sec) | Position Angle (deg) |
| 4.00 ± 0.05 | 16.7 ± 0.5 | -16.23 | 1 | 1.20 ± 0.30 | 4.2 ± 0.9 | -14.4 ± 1.0 | 0.0 ± 1.0 | 0.68 ± 0.34 | 2.6 ± 1.9 | 36,322 | 49 | -10.4 ± 3.9 | 1.6 ± 1.2 | -9.3 ± 3.9 | 1.4 ± 1.2 | 9.4 ± 3.9 | 278.6 ± 8.2 |
| | | | 2 | 1.00 ± 0.30 | 4.4 ± 1.0 | -12.2 ± 1.0 | -2.6 ± 1.0 | 0.63 ± 0.34 | 2.9 ± 1.7 | 33,219 | 54 | | | | | | |
| | | | 3 | 0.15 ± 0.05 | 3.3 ± 0.5 | 9.1 ± 1.0 | 0.0 ± 1.6 | 0.05 ± 0.02 | 0.0 ± 1.4 | 2,802 | 45 | | | | | | |
| | | | 4 | 0.30 ± 0.10 | 3.8 ± 0.4 | 13.2 ± 0.5 | -2.8 ± 0.5 | 0.14 ± 0.06 | 1.9 ± 0.9 | 7,433 | 39 | | | | | | |
| | | | 5 | 0.30 ± 0.10 | 4.0 ± 0.5 | 0.4 ± 0.5 | 3.4 ± 0.5 | 0.16 ± 0.07 | 2.3 ± 0.9 | 8,236 | 41 | | | | | | |
| | | | 6 | 0.10 ± 0.05 | 5.4 ± 1.0 | 9.2 ± 1.0 | 4.4 ± 1.0 | 0.09 ± 0.06 | 4.3 ± 1.3 | 5,003 | 62 | | | | | | |
| | | | 7 | 0.50 ± 0.10 | 3.9 ± 0.3 | -9.6 ± 0.5 | 9.4 ± 0.5 | 0.25 ± 0.06 | 2.1 ± 0.6 | 13,049 | 25 | | | | | | |
| | | | 8 | 0.25 ± 0.20 | 3.3 ± 0.1 | -10.3 ± 1.4 | -2.1 ± 1.6 | 0.09 ± 0.07 | 0.0 ± 0.7 | 4,671 | 80 | | | | | | |
| | | | 9 | 0.20 ± 0.15 | 4.6 ± 1.0 | -1.4 ± 1.4 | 12.0 ± 1.6 | 0.14 ± 0.12 | 3.2 ± 1.5 | 7,261 | 86 | | | | | | |

## REFERENCES

1. Kundu, M.R., "Solar Radio Astronomy," New York:Wiley, 1965

   a. pp. 168-170

   b. p. 220

2. Allen, C.W., "Astrophysical Quantities," 2nd Edition, University of London: Althone Press, 1963

   a. p. 184

   b. p. 188

3. Tsuchiya, A., and Nagame, K., "Observations of the S-Component of the Solar Radio Emission by an Eight Element Grating Interferometer at 17 Gc/s," Solar Physics 1:121 (1967) (Journal published by D. Reidel Publishing Co., Dordrecht, Holland)

4. Takakura, T., "Theory of Solar Bursts," Solar Physics 1(No. 3/4):304 (1967)

5. McClain, E.F., "A High-Precision 85-Foot Radio Telescope," Sky and Telescope 32(No. 1):4 (1966)

## Appendix A

## COMPUTER PROGRAM FOR DATA REDUCTION

```
      PROGRAM SUN 2
      DIMENSION T(20),W(20),RA(20),DEC(20),ET(20),EW(20),ERA(20),EDEC(20
     1),S(20),C(20),EC(20),ES(20),EWS(20)
      RADM= 57.29578
  101 FORMAT(3I2,F6.2,F5.1,F6.2,I2,F6.2,F5.1)
  102 FORMAT(F6.2,3F5.1,F6.2,4F5.1)
  103 FORMAT(1H1/)
  104 FORMAT(9X,13H SUN DATA ON ,I2,1H-,I2,1H-,I2,42H AT 14.50-GC/S USIN
     1G 85-FT MD PT TELESCOPE/)
  105 FORMAT(9X,43H SUN DEFL ERR  SUN RAD ERR       AVG SUN DEC)
  106 FORMAT(9X,F9.2,F4.2,4X,F5.1,F4.1,4H MIN,3X,F6.2,4H DEG/)
  107 FORMAT(9X,14H THE FOLLOWING,I3,22H HOTSPOTS WERE PRESENT/)
  108 FORMAT(9X,20H MEASURED QUANTITIES)
  109 FORMAT(9X,23HN  DEFL  ERR  WIDTH ERR,7X,7HRA  ERR,7X,7HDEC ERR)
  110 FORMAT(8X,I2,F6.2,F5.2,F7.1,F4.1,4H MIN,F6.1,F4.1,4H MIN,F6.1,F4.1
     1,4H MIN)
  111 FORMAT(1H0)
  112 FORMAT(9X,31H COMPUTED QUANTITIES AND ERRORS)
  113 FORMAT(9X,27HN FLUX/FLUX-QUIET-SUN  SIZE,10X,4HFLUX,9X,3HERR)
  114 FORMAT(8X,I2,F6.2,F5.2,8H PERCENT,F6.1,F4.1,4H MIN,I8,7H JANSKY,I4
     1,8H PERCENT)
  115 FORMAT(10X,65HPOSITION OF BRIGHTNESS CENTROID RELATIVE TO SUNS GEO
     1METRIC CENTER)
  116 FORMAT(20X,6HRA ERR,11X,7HDEC ERR)
  117 FORMAT(17X,F5.1,F4.1,7H ARCSEC,2X,F5.1,F4.1,7H ARCSEC/)
  118 FORMAT(9X,58H CENTROID AT 15.375-GC/S USING SPECTRAL CORRECTION OF
     1 0.89)
  119 FORMAT(10X,39HCENTROID EXPRESSED IN POLAR COORDINATES/)
  120 FORMAT(16X,11HRADIUS  ERR,10X,13HPOS ANG   ERR)
  121 FORMAT(15X,2F6.1,7H ARCSEC,4X,2F6.1,8H DEGREES)
 1000 READ101,NMON,NDAY,NYEAR,TS,RS,DECS,NS,ETS,ERS
      IF(EOF,60)500,100
  100 DO 1 J=1,NS
      READ102,T(J),W(J),RA(J),DEC(J),ET(J),WX,WI,ERA(J),EDEC(J)
      RA(J)=(RA(J)*COSF(DECS/RADM))/4.0
      ERA(J)=(ERA(J)*COSF(DECS/RADM))/4.0
      EW(J)=(WX-WI)/2.0
      EWS(J)=0.5*(SQRTF(WX*WX-10.89)-SQRTF(WI*WI-10.89))
    1 S(J)=(T(J)*W(J)*W(J))/(2.7724*TS*RS*RS)
      R=0
      D=0
      ST=0
      ECRA=0
      ECDEC=0
      DO 2 J=1,NS
      R=R+S(J)*RA(J)
      D=D+S(J)*DEC(J)
      ST=ST+S(J)
      ES(J)=(S(J)**2)*((ET(J)/T(J))**2+(ETS/TS)**2+(2*ERS/RS)**2+(2*EW(J
     1)/W(J))**2)
      ECRA=ECRA+ES(J)*(RA(J)**2)+(S(J)**2)*(ERA(J)**2)
      ECDEC=ECDEC+ES(J)*(DEC(J)**2)+(S(J)**2)*(EDEC(J)**2)
    2 ES(J)=SQRTF(ES(J))
      ST=1+ST
      CR=(60*R)/ST
      CD=(60*D)/ST
```

```
      ECR=60*SQRTF(ECRA/(ST*ST))
      ECD=60*SQRTF(ECDEC/(ST*ST))
      PRINT103
      PRINT104,NMON,NDAY,NYEAR
      PRINT105
      PRINT106,TS,ETS,RS,ERS,DECS
      PRINT107,NS
      PRINT108
      PRINT109
      DO 3 J=1,NS
    3 PRINT110,J,T(J),ET(J),W(J),EW(J),RA(J),ERA(J),DEC(J),EDEC(J)
      PRINT111
      PRINT112
      PRINT113
      DO 4 J=1,NS
      NFLX=(10.68*11950/6.83)*T(J)*((W(J)/3.3)**2)
      NEFLX=100*SQRTF((ET(J)/T(J))**2+0.0025+(2*EW(J)/W(J))**2)
      S(J)=100*S(J)
      ES(J)=100*ES(J)
      W(J)=SQRTF(W(J)*W(J)-10.89)
    4 PRINT 114,J,S(J),ES(J),W(J),EWS(J),NFLX,NEFLX
      PRINT111
      PRINT115
      PRINT116
      PRINT117,CR,ECR,CD,ECD
      PRINT118
      PRINT116
      CR=0.89*((60*R)/ST)
      CD=0.89*((60*D)/ST)
      PRINT117,CR,ECR,CD,ECD
      CP=SQRTF(CR*CR+CD*CD)
      CA=RADM*ATANF(CR/CD)
      ECP=(SQRTF((CR*ECR)**2+(CD*ECD)**2))/CP
      ECA=(RADM/(CP**2))*(SQRTF((CR*ECD)**2+(CD*ECR)**2))
      IF(CD)5,6,6
    5 CA=CA+180
      GO TO 8
    6 IF(CR)7,8,8
    7 CA=CA+360
    8 PRINT119
      PRINT120
      PRINT121,CP,ECP,CA,ECA
      GO TO 1000
  500 END
```

Security Classification

## DOCUMENT CONTROL DATA - R & D

*(Security classification of title, body of abstract and indexing annotation must be entered when the overall report is classified)*

| | |
|---|---|
| 1. ORIGINATING ACTIVITY *(Corporate author)*<br>Naval Research Laboratory<br>Washington, D.C. 20390 | 2a. REPORT SECURITY CLASSIFICATION<br>Unclassified<br>2b. GROUP |

3. REPORT TITLE

MEASUREMENTS OF THE SOLAR BRIGHTNESS DISTRIBUTION AT 14.50 GHZ

4. DESCRIPTIVE NOTES *(Type of report and inclusive dates)*

A final report on one phase of the problem; work continues on the problem.

5. AUTHOR(S) *(First name, middle initial, last name)*

James P. Hollinger

| | | |
|---|---|---|
| 6. REPORT DATE<br>June 6, 1968 | 7a. TOTAL NO. OF PAGES<br>20 | 7b. NO. OF REFS<br>5 |
| 8a. CONTRACT OR GRANT NO.<br>NRL Problem A01-35<br>b. PROJECT NO.<br>S-3404, Task 4896<br>c.<br>d. | 9a. ORIGINATOR'S REPORT NUMBER(S)<br>NRL Report 6692<br>9b. OTHER REPORT NO(S) *(Any other numbers that may be assigned this report)* | |

10. DISTRIBUTION STATEMENT

This document has been approved for public release and sale; its distribution is unlimited.

| | |
|---|---|
| 11. SUPPLEMENTARY NOTES | 12. SPONSORING MILITARY ACTIVITY<br>Department of the Navy<br>(Naval Ship Systems Command),<br>Washington, D.C. 20360 |

13. ABSTRACT

Observations of the solar brightness distribution at 14.50 GHz have been made using the NRL 85-ft reflector. The apparent angular size, intensity, and relative position of the active regions present on the solar disk were measured on six different days. These measurements were used to compute the radio brightness centroid relative to the geometrical center of the solar disk and the flux and size of the active regions. Spectral corrections were applied to the data to derive the brightness centroid at 15.375 GHz.

DD FORM 1 NOV 65 1473 (PAGE 1)

S/N 0101-807-6801



Security Classification

| 14. KEY WORDS | LINK A ROLE | LINK A WT | LINK B ROLE | LINK B WT | LINK C ROLE | LINK C WT |
|---|---|---|---|---|---|---|
| Radio astronomy | | | | | | |
| Sun | | | | | | |
| Radiation | | | | | | |
| Brightness distribution | | | | | | |
| Brightness centroid | | | | | | |